

# Honokiol traverses the blood-brain barrier and induces apoptosis of neuroblastoma cells via an intrinsic bax-mitochondrion-cytochrome c-caspase protease pathway

Jia-Wei Lin, Juei-Tai Chen, Chung-Ye Hong, Yi-Ling Lin, Kuan-Ting Wang, Chih-Jung Yao, Gi-Ming Lai, and Ruei-Ming Chen

*Department of Neurosurgery, Taipei Medical University-Shuang Ho Hospital (J.-W.L.); Brain Disease Research Center (J.-T.C., Y.-L.L., R.M.C.); Department of Internal Medicine, Taipei Medical University-Wan-Fang Hospital (C.-Y.H.); Graduate Institute of Medical Sciences (K.-T.W., R.-M.C.); Center of Excellence for Cancer Research (C.-J.Y., G.-M.L., R.-M.C.), Taipei Medical University, Taipei, Taiwan*

Neuroblastomas, an embryonic cancer of the sympathetic nervous system, often occur in young children. Honokiol, a small-molecule polyphenol, has multiple therapeutic effects and pharmacological activities. This study was designed to evaluate whether honokiol could pass through the blood-brain barrier (BBB) and induce death of neuroblastoma cells and its possible mechanisms. Primary cerebral endothelial cells (CECs) prepared from mouse brain capillaries were cultured at a high density for 4 days, and these cells formed compact morphologies and expressed the ZO-1 tight-junction protein. A permeability assay showed that the CEC-constructed barrier obstructed the passing of FITC-dextran. Analyses by high-performance liquid chromatography and the UV spectrum revealed that honokiol could traverse the CEC-built junction barrier and the BBB of ICR mice. Exposure of neuroblastoma neuro-2a cells and NB41A3 cells to honokiol induced cell shrinkage and decreased cell viability. In parallel, honokiol selectively induced DNA fragmentation and cell apoptosis rather than cell necrosis. Sequential treatment of neuro-2a cells with honokiol increased the expression of the proapoptotic Bax protein and its translocation from the cytoplasm to mitochondria. Honokiol successively decreased the mitochondrial membrane potential but increased the release of cytochrome c from mitochondria.

Consequently, honokiol induced cascade activation of caspases-9, -3, and -6. In comparison, reducing caspase-6 activity by Z-VEID-FMK, an inhibitor of caspase-6, simultaneously attenuated honokiol-induced DNA fragmentation and cell apoptosis. Taken together, this study showed that honokiol can pass through the BBB and induce apoptotic insults to neuroblastoma cells through a Bax-mitochondrion-cytochrome c-caspase protease pathway. Therefore, honokiol may be a potential candidate drug for treating brain tumors.

**Keywords:** apoptosis, blood-brain barrier, honokiol, neuroblastoma, signal-transducing events.

Childhood cancer remains the leading cause of disease-related death in children.<sup>1</sup> Neuroblastomas, an embryonal cancer of the sympathetic nervous system, often occur in young children.<sup>2</sup> Clinically, children with a neuroblastoma are usually designated as high-risk patients.<sup>3</sup> Thus, neuroblastomas are a major problem in pediatric oncology. Current treatment for neuroblastomas with adverse prognostic features consists of a coordinated sequence of chemotherapy, surgery, and radiation.<sup>4</sup> Noteworthy improvements in outcomes of these patients with neuroblastoma were achieved with an intensification of conventional chemotherapy. Meanwhile, lots of children with a high-risk neuroblastoma may achieve a long-term cure or possibly develop complications, including hearing loss, cardiac dysfunction, infertility, and second malignancies.<sup>5,6</sup> Treatment failures usually arise from the setting of minimal residual disease following high-dose chemotherapy.<sup>7</sup> Therefore, more-effective

Received June 15, 2011; accepted November 11, 2011.

**Corresponding Author:** Ruei-Ming Chen, PhD, Graduate Institute of Medical Sciences, College of Medicine, Taipei Medical University, 250 Wu-Hsing St, Taipei 110, Taiwan (rmchen@tmu.edu.tw).

and less-toxic therapies, including the targeting of tumor cells in a more selective and efficient way to improve survival, need to be developed.

Developing unconventional biologic antitumor drugs may benefit therapy of neuroblastomas. Matthay et al (1999) first demonstrated that administration of 13-cis-retinoic acid following recovery from high-dose chemotherapy and stem-cell transplantation improved the 3-year event-free survival of patients with high-risk neuroblastomas.<sup>8</sup> Honokiol (2-(4-hydroxy-3-prop-2-enyl-phenyl)-4-prop-2-enyl-phenol), a small-molecule polyphenol, is one of the main physiologically bioactive constituents of the traditional Chinese medicine Houpo (*Magnolia officinalis* Rehd. et Wils.), which was proven to be effective in treating a variety of diseases, such as anxiety and nervous disturbances, thrombotic stroke, typhoid fever, and dead muscles.<sup>9,10</sup> As a newly identified natural retinoid, honokiol was shown to activate the retinoid X receptor, resulting in the induction of ATP-binding cassette transporter A1 messenger (m)RNA and protein expression.<sup>11</sup> In addition, honokiol has multiple therapeutic effects and pharmacological activities, such as anti-anxiety, antidepressant, antioxidant, anti-inflammation, antibacteria, antiplatelet, and anti-arrhythmia functions.<sup>12,13</sup> Being a neuroactive compound, honokiol can promote neurite outgrowth in primary cultured rat cortical neurons through activating extracellular signal-regulated kinases.<sup>14</sup> In addition, honokiol has neuroprotective effects against oxidative stress-induced neuronal damage.<sup>15</sup> Recently, honokiol was reported to have anti-angiogenic, anti-inflammatory, and antitumor properties in preclinical models but did not induce appreciable toxicity.<sup>13,16</sup>

Therapeutic options for treating malignant brain tumors are limited because of the presence of the blood-brain barrier (BBB).<sup>17</sup> The BBB plays important roles in maintaining homeostasis of the cerebral microenvironment.<sup>18,19</sup> Cerebral endothelial cells (CECs) form complex tight junctions in the BBB to force most molecular traffic to take a transcellular route across the barrier.<sup>19,20</sup> Targeting death receptor-mediated apoptosis has emerged as an effective strategy for cancer therapy.<sup>21</sup> A variety of intrinsic and extrinsic factors contribute to regulation of cell apoptosis.<sup>22,23</sup> Bax, a proapoptotic protein, functions as an essential gateway that mediates mitochondrion-dependent apoptosis.<sup>24</sup> Bax translocated from the cytoplasm to mitochondria can permeabilize the outer membrane, which then triggers the release of cytochrome (Cyt) c and reactive oxygen species.<sup>25</sup> Then, Cyt c can stimulate cascade activation of caspases-9, -3, and -6, leading to cleavage of key cellular proteins and consequent damage to genomic DNA.<sup>26</sup> Previous studies reported that honokiol combined with cisplatin or a tumor necrosis factor-related apoptosis-inducing ligand can induce apoptosis of human lung cancer.<sup>21,27</sup> Meanwhile, the effects of honokiol on neuroblastoma cells are still unknown. Therefore, in this study, we evaluated whether honokiol could pass through the BBB to induce cytotoxicity to neuroblastoma cells and its possible molecular mechanisms.

## Materials and Methods

### Cell Culture and Drug Treatment

Neuroblastoma neuro-2a cells and NB41A3 cells purchased from American Type Culture Collection were cultured in Dulbecco's modified Eagle's medium (DMEM; Gibco-BRL) supplemented with 10% heat-inactivated fetal bovine serum (FBS), L-glutamine, 100 IU/mL penicillin, and 100 µg/mL streptomycin in 75-cm<sup>2</sup> flasks at 37°C in a humidified atmosphere of 5% CO<sub>2</sub>. Human astrocytes (HA-h) from ScienCell Research Laboratories were cultured in astrocyte medium (ScienCell Research Laboratories). Cells were grown to confluence prior to ketamine administration. Honokiol was purchased from Sigma, and its purity was >98%. Honokiol was freshly dissolved in dimethyl sulfoxide (DMSO). Neuroblastoma cells were exposed to different concentrations of honokiol for various intervals.

### Isolation of Mouse CECs

Mouse CECs were prepared from cerebral capillaries according to a previously described method.<sup>28</sup> This investigation conformed to the *Guide for the Care and Use of Laboratory Animals* published by the US National Institutes of Health (NIH publication no. 85-23, revised 1996), and all procedures were pre-approved by the Institutional Animal Care and Use Committee of Taipei Medical University, Taipei, Taiwan. Mouse CECs were seeded in DMEM supplemented with 10% heat-inactivated FBS, L-glutamine, penicillin (100 IU/mL), and streptomycin (100 µg/mL) in 75-cm<sup>2</sup> flasks at 37°C in a humidified atmosphere of 5% CO<sub>2</sub>. To verify that the isolated brain cells were CECs in our preparation, immunocytochemical analyses of vimentin and factor VIII were performed in accordance with the standard protocol provided with the VectaStain ABC kit (Vector Laboratories), as described previously.<sup>29</sup> Cells were grown to confluence prior to drug treatment. Only the first 10 passages of mouse CECs were used in this study.

### Construction of CEC Tight Junctions

CECs ( $5 \times 10^4$  cells/cm<sup>2</sup>) were seeded in Transwell cell culture chamber inserts (Corning Costar) for 4 days. The ZO-1 tight-junction structure was immunostained and observed using confocal microscopy, as described previously.<sup>30</sup> Permeability of CEC monolayers was determined using fluorescein isothiocyanate (FITC)-labeled dextran (Molecular Probes) as the penetrating chemical.<sup>31</sup> In brief, the medium containing 1 µg/µL FITC-labeled dextran was added to top chambers and incubated for 2 h. Then, the medium from the bottom chambers was collected and centrifuged, and the supernatant was analyzed using fluorescence spectrophotometry.

### *Determination of Honokiol's Transport Through CEC Tight Junctions*

CECs ( $10^6$  cells) were seeded in Transwell cell culture chamber inserts (Corning Costar) for 4 days to form the tight-junction barrier. Honokiol was added to the top chambers for 0.5, 1, and 3 h. After drug treatment, the medium from the bottom chambers was collected and extracted with cyclohexane. Following centrifugation, the organic layers containing honokiol were dried under nitrogen. The extracted products were dissolved in 200  $\mu$ L of the mobile phase (65% acetonitrile, 35% water, and 0.07% acetic acid) and then applied for analysis by high-performance liquid chromatography (HPLC; 600S and 717plus; Waters) as described previously.<sup>32</sup> The UV spectra of the measured and standard honokiol were analyzed using a photodiode array detector (PDA 996; Waters).

### *Animal Treatment*

All procedures were performed according to the National Institutes of Health Guidelines for the Use of Laboratory Animals and approved by the Institutional Animal Care and Use Committee of Taipei Medical University, Taipei, Taiwan. Male ICR mice (20–25 g;  $n = 6$ ) were purchased from the Animal Center of the College of Medicine, National Taiwan University, Taipei, Taiwan. The animals were intravenously injected with honokiol at 25 mg/kg body weight for 15 and 30 min. After perfusion to remove honokiol residuals in the vessels, the animals were killed, and the brain tissues were collected. Following homogenization, the homogenates were extracted with acetonitrile for HPLC analysis of honokiol.

### *Cytotoxic Assay*

Analyses of cell morphologies and viability were performed to determine the toxicity of honokiol to neuroblastoma cells. Neuro-2a cells ( $10^4$  cells) were cultured in 96-well tissue culture plates (Corning Costar) for 12 h and then treated with 2.5, 5, 10, 20, 30, 40, 50, 60, 80, and 100  $\mu$ M honokiol for 72 h. Cell morphologies were observed and photographed using a light microscope. Cell viability was assayed by a colorimetric method.<sup>33</sup> After drug treatment, neuroblastoma cells were cultured with new medium containing 500  $\mu$ g/L 3-(4,5-dimethylthiazol-2-yl)-2,5-diphenyltetrazolium bromide (Sigma) for another 3 h. The formazan product was dissolved in dimethyl sulfoxide and spectrophotometrically measured, and the 50% lethal concentration ( $LC_{50}$ ) was determined. Effects of honokiol on viabilities of mouse CECs, human HA-h astrocytes, and neuroblastoma NB41A3 cells were also determined.

### *Quantification of Necrotic Cells*

Necrotic cells were quantified using a photometric immunoassay according to a previously described

method.<sup>34</sup> In brief, neuroblastoma cells ( $10^5$  cells) were seeded in 96-well tissue culture plates overnight. After honokiol administration, cell lysates and culture medium were collected, and necrotic cells were immunodetected using mouse monoclonal antibodies (mAbs) against histone. After an antibody reaction and washing, the colorimetric product was measured at 405 nm against a substrate solution as a blank.

### *Quantification of DNA Fragmentation*

DNA fragmentation in neuroblastoma cells was quantified using a cellular DNA fragmentation enzyme-linked immunosorbent assay (ELISA) kit (Boehringer Mannheim), as described previously.<sup>35</sup> In brief, neuroblastoma cells ( $2 \times 10^5$  cells) were subcultured in 24-well tissue culture plates and labeled with BrdU overnight. Cells were harvested and suspended in the culture medium. One hundred microliters of the cell suspension was added to each well of 96-well tissue culture plates. Neuroblastoma cells were cocultured with honokiol for another 8 h at 37°C in a humidified atmosphere of 5% CO<sub>2</sub>. Amounts of BrdU-labeled DNA in the cytoplasm were quantified using an Anthos 2010 microplate photometer (Anthos Labtec Instruments) at a wavelength of 450 nm.

### *Analysis of Apoptotic Cells*

Apoptosis of neuroblastoma cells was determined using propidium iodide to detect DNA injury in nuclei according to a previously described method.<sup>36</sup> After drug administration, neuroblastoma cells were harvested and fixed in cold 80% ethanol. After centrifugation and washing, fixed cells were stained with propidium iodide and analyzed using a FACScan flow cytometer (Becton Dickinson).

### *Confocal Microscopic Analysis of Bax Translocation*

Bax in neuroblastoma cells was recognized by a specific antibody and visualized using confocal microscopy according to a previously described method.<sup>37</sup> In brief, after drug treatment, neuroblastoma cells were fixed with a fixing reagent (acetone:methanol, 1:1) at  $-20^\circ\text{C}$  for 10 min. Following rehydration, cells were incubated with 0.2% Triton X-100 at room temperature for 15 min. The mouse mAb used in this study was generated against human Bax (Santa Cruz Biotechnology). Immunodetection of Bax in neuroblastoma cells was performed at 4°C overnight. After washing, cells were sequentially reacted with second antibodies and biotin-SP-conjugated AffiniPure goat anti-rabbit immunoglobulin G (IgG; Jackson ImmunoResearch) at room temperature for 1 h. After washing, the third antibody with Cy3-conjugated streptavidin (Jackson ImmunoResearch) was added to neuroblastoma cells and reacted at room temperature for 30 min. Mitochondria of fixed neuroblastoma cells were stained with 3,3'-dihexyloxycarbocyanine (DiOC<sub>6</sub>;

Molecular Probes), a positively charged dye, at 37°C for 30 min. A confocal laser scanning microscope (Model FV500; Olympus) was used for sample observation. Illumination for the existence of Bax protein was demonstrated by the appearance of hot spots in both the cytoplasm (red signals) and membranes (yellow signals). Images were acquired and quantified using FluoView software (Olympus).

#### *Quantification of the Mitochondrial Membrane Potential*

The mitochondrial membrane potential was determined using a previously described method.<sup>38</sup> In brief, neuroblastoma cells ( $5 \times 10^5$  cells) were seeded in 12-well tissue culture plates overnight and then treated with drugs. After drug administration, neuroblastoma cells were harvested and incubated with DiOC<sub>6</sub> at 37°C for 30 min in a humidified atmosphere of 5% CO<sub>2</sub>. After washing and centrifugation, cell pellets were suspended in phosphate-buffered saline (0.14 M NaCl, 2.6 mM KCl, 8 mM Na<sub>2</sub>HPO<sub>4</sub>, and 1.5 mM KH<sub>2</sub>PO<sub>4</sub>). Intracellular fluorescent intensities were analyzed using a flow cytometer (FACS Calibur).

#### *Gel Electrophoresis and Immunoblotting Analysis*

Protein analyses were performed according to a previously described method.<sup>39</sup> After drug treatment, neuroblastoma cells were washed with 1× phosphate-buffered saline. Cell lysates were prepared in ice-cold radioimmunoprecipitation assay buffer (25 mM Tris-HCl [pH, 7.2], 0.1% sodium dodecylsulfate, 1% Triton X-100, 1% sodium deoxycholate, 0.15 M NaCl, and 1 mM EDTA). To avoid protein degradation, a mixture of proteinase inhibitors, including 1 mM phenyl methyl sulfonyl fluoride, 1 mM sodium orthovanadate, and 5 µg/mL leupeptin, was added to the radioimmunoprecipitation assay buffer. Protein concentrations were quantified using a bicinchoninic acid protein assay kit (Pierce). Cytosolic proteins (100 µg per well) were subjected to sodium dodecylsulfate polyacrylamide gel electrophoresis and transferred to nitrocellulose membranes. Membranes were blocked with 5% nonfat milk at 37°C for 1 h. Immunodetection of Cyt c was performed using a mouse mAb against rat Cyt c (Transduction Laboratories). Cellular β-actin protein was immunodetected using a mouse mAb against mouse β-actin (Sigma) as an internal standard. Intensities of the immunoreactive bands were determined using an UVIDOCMW, version 99.03, digital imaging system (UVtec).

#### *Fluorogenic Substrate Assay for Caspase Activities*

Activities of caspase-3, -6, and -9 in neuroblastoma cells were determined using fluorometric assay kits (R&D Systems), as described previously.<sup>40</sup> In brief, after honokiol administration, neuroblastoma cells were lysed using a buffer containing 1% Nonidet

P-40, 200 mM NaCl, 20 mM Tris/HCl (pH, 7.4), 10 µg/mL leupeptin, 0.27 U/mL aprotinin, and 100 µM PMSF. Cell extracts (25 µg total protein) were incubated with 50 µM specific fluorogenic peptide substrates in 200 µL of a cell-free system buffer composed of 10 mM HEPES (pH, 7.4), 220 mM mannitol, 68 mM sucrose, 2 mM NaCl, 2.5 mM KH<sub>2</sub>PO<sub>4</sub>, 0.5 mM EGTA, 2 mM MgCl<sub>2</sub>, 5 mM pyruvate, 0.1 mM PMSF, and 1 mM dithiothreitol. The peptide substrates for assays of caspase-3, -6, and -9 activities were DEVD, VEID, and LEHD, respectively. These peptides were conjugated to 7-amino-4-trifluoromethyl coumarin for fluorescence detection. For an inhibition assay, neuro-2a cells were pretreated with 50 µM Z-VEID-FMK, an inhibitor of caspase-6, for 1 h and then exposed to honokiol. Intensities of the fluorescent products were measured using an LS 55 spectrometer from PerkinElmer Instruments.

#### *Statistical Analysis*

One-way repeated-measure analysis of variance with Duncan's multiple-range post-hoc test was used to compare cell viability, permeability, necrosis, DNA fragmentation, apoptosis, mitochondrial membrane potential, Cyt c release, and caspase activities in response to treatments with different concentrations of honokiol for various intervals. Values in the text are the mean ± standard error of the mean. Differences were considered to be statistically significant at  $P < .05$ .

## Results

#### *Honokiol Can Pass Through the CEC-Constructed Tight-Junction Barrier and the BBB*

After culturing CECs in transwells at a high density for 4 days, cells grew into compact morphologies (Fig. 1A). Furthermore, confocal analysis revealed that after such culture conditions, CECs expressed ZO-1 protein and formed a tight junction barrier (Fig. 1A). Results of the permeability assay showed that dextran-FITC, a complex branched glucan, could not cross the CEC tight-junction barrier in untreated groups (Fig. 1B). Exposure to 40 µM honokiol for 0.5, 1, and 24 h did not affect the permeability. Meanwhile, the HPLC analysis revealed that honokiol was detected in the bottom medium (Fig. 1C). A spectral analysis revealed that the measured honokiol had the same UV spectrum as the standard one (Fig. 1D and E). When honokiol was added to the upper layer of the transwells, the passing of this polyphenol across the CEC tight-junction barrier was augmented in a time-dependent manner (Fig. 1F). After intravenous injection of honokiol into ICR mice for 15 and 30 min, this compound could be time-dependently detected in the brain tissues (Fig. 1G).



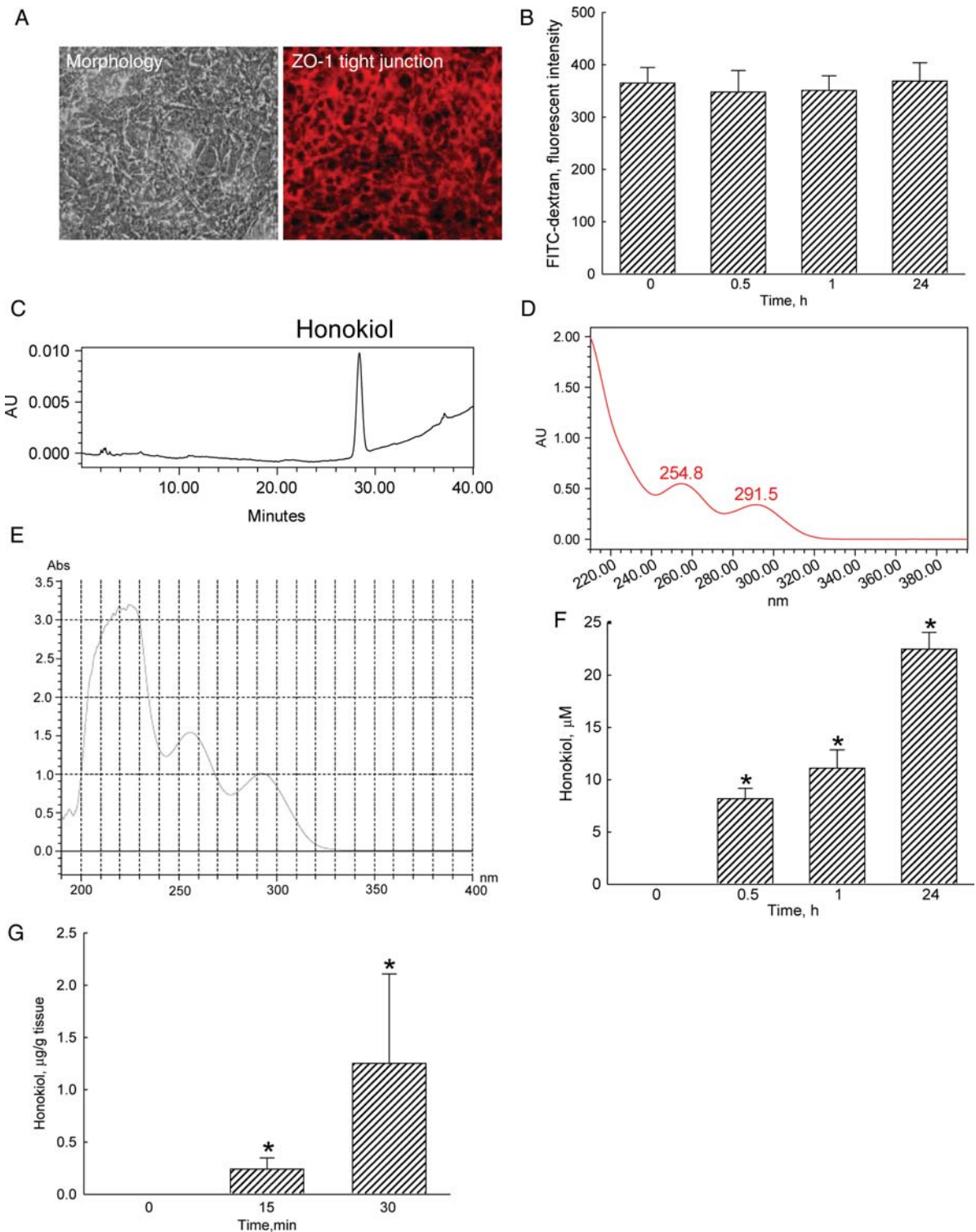


Fig. 1. Effects of honokiol on passing through the cerebral endothelial cell (CEC)-constructed tight-junction barrier. CECs isolated from mouse brain tissues were seeded in Transwell cell culture chamber inserts at a high density ( $5 \times 10^4$  cells/cm<sup>2</sup>) for 4 days. Cell morphology was observed and photographed using a reverse-phase microscope (A, right panel). The ZO-1 tight-junction structure was immunostained and observed using confocal microscopy (left panel). Permeability of the CEC monolayer was determined using FITC-labeled dextran (B). Honokiol (40  $\mu\text{M}$ ) was added to the upper chamber for various time intervals. The bottom medium was collected for an HPLC analysis (C). The UV spectra of isolated (D) and standard (E) honokiol were analyzed using a photodiode array detector. The passing of honokiol through the tight junction barrier was quantified (F). ICR mice were intravenously injected with honokiol for 15 and 30 min, and the passing of honokiol through the BBB of ICR mice was evaluated (G). Each value represents the mean  $\pm$  standard error of the mean for  $n = 6$ . \*The value significantly differs from the respective control,  $P < .05$ .

### Honokiol Induces Death of Neuroblastoma Cells in Concentration- and Time-Dependent Manners

Treatment of neuro-2a cells with 2.5, 5, 10, 20, 30, 40, 50, 60, 80, and 100  $\mu\text{M}$  honokiol for 72 h decreased cell numbers and caused cell shrinkage (Fig. 2A). Analysis of cell viability further showed that the  $\text{LC}_{50}$  of honokiol was 63.3  $\mu\text{M}$  (Fig. 2B). Exposure of neuro-2a cells to 40  $\mu\text{M}$  honokiol for 24, 48, and 72 h decreased cell numbers and caused morphological shrinkage (Fig. 3A). After treatment with 40  $\mu\text{M}$  honokiol for 24, 48, and 72 h, the viability of neuro-2a cells was reduced by 23%, 32%, and 44%, respectively (Fig. 3B).

### Honokiol Selectively Induces Apoptosis but not Necrosis of Neuroblastoma Cells

Analyses of necrotic cells revealed that treatment of neuro-2a cells with 40  $\mu\text{M}$  honokiol for 24, 48, and 72 h did not cause cell necrosis (Fig. 4A). Meanwhile, exposure to 40  $\mu\text{M}$  honokiol for 24 h caused a significant 3.1-fold increase in DNA fragmentation (Fig. 4B). When the treated intervals reached 48 and 72 h, honokiol induced DNA fragmentation of neuro-2a cells by 5.6- and 9.7-fold, respectively. Analysis of the cell cycle showed that treatment of neuro-2a cells with 40  $\mu\text{M}$  honokiol for 24 h caused a significant 19% induction of cell apoptosis (Fig. 4C). After exposure for

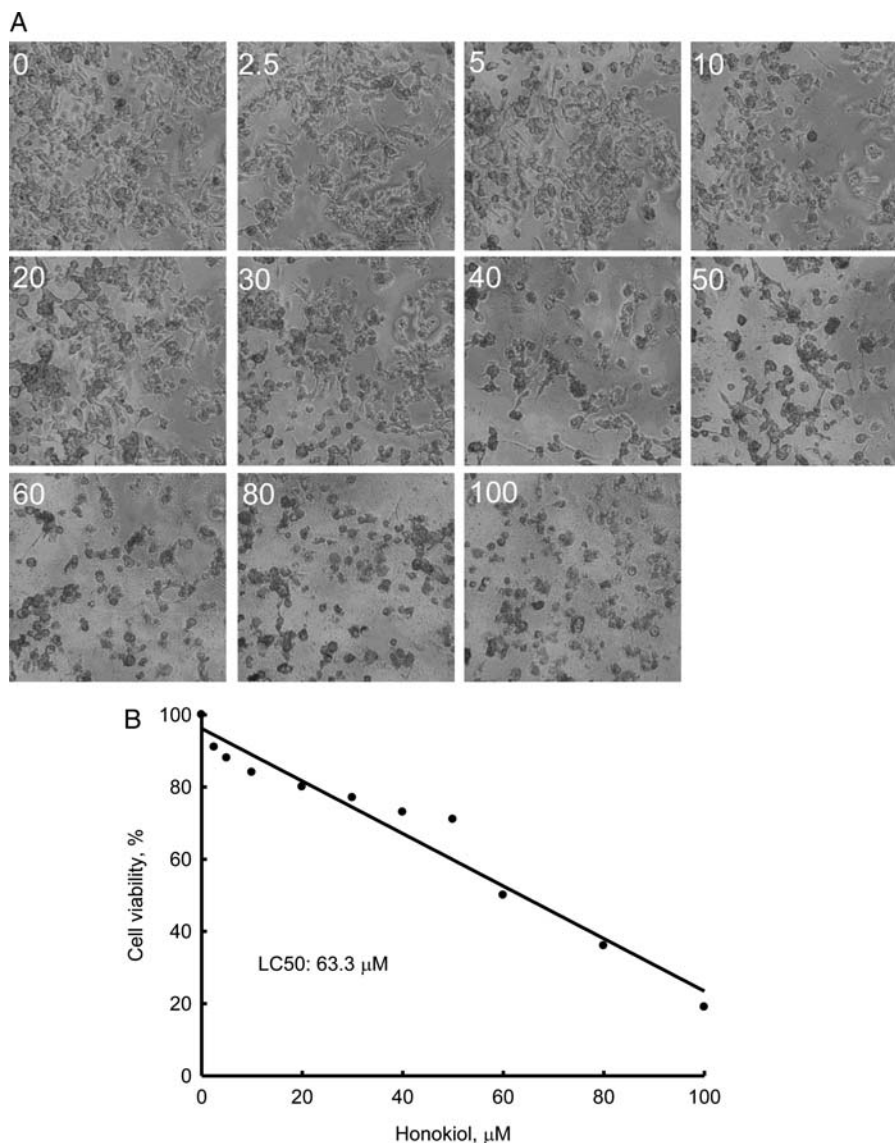


Fig. 2. Concentration-dependent effects of honokiol on the death of neuroblastoma cells. Neuro-2a cells were treated with 2.5, 5, 10, 20, 30, 40, 50, 60, 80, and 100  $\mu\text{M}$  honokiol for 3 days. Cell morphologies were observed and photographed using a reverse-phase microscope (A). Cell viability was assayed using a colorimetric method (B). Each value represents the mean  $\pm$  standard error of the mean for  $n = 6$ .

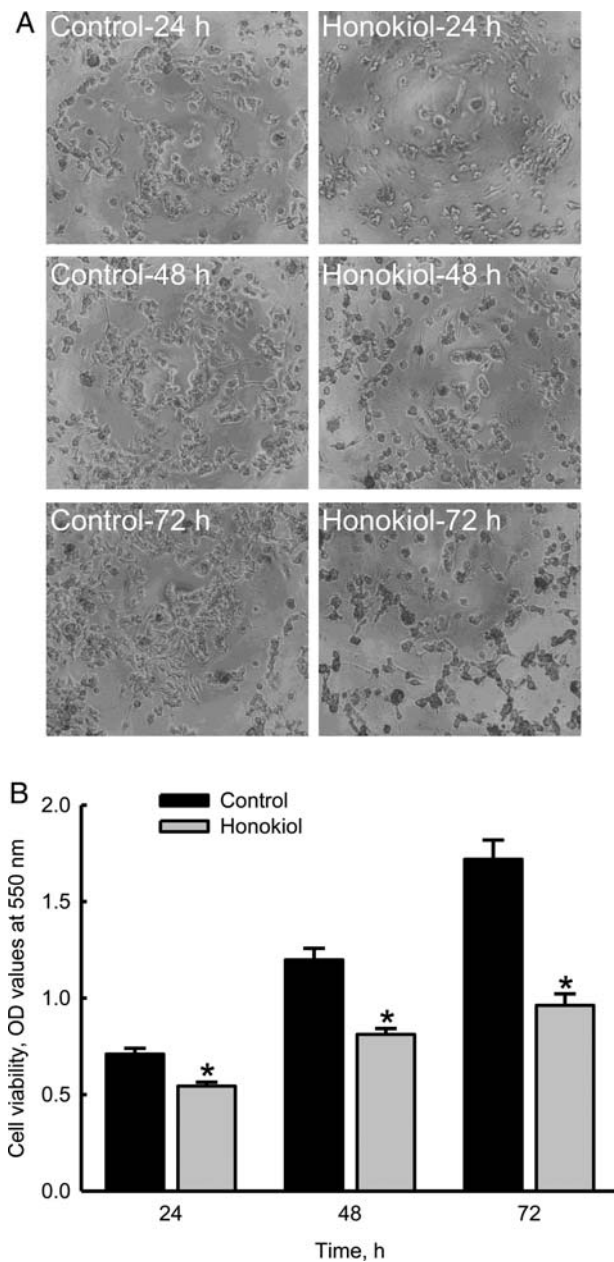


Fig. 3. Time-dependent effects of honokiol on the death of neuroblastoma cells. Neuro-2a cells were treated with 40  $\mu$ M honokiol for 24, 48, and 72 h. Cell morphologies were observed and photographed using a reverse-phase microscope (A). Cell viability was assayed using a colorimetric method (B). Each value represents the mean  $\pm$  standard error of the mean for  $n = 6$ . \*The value significantly differs from the respective control,  $P < .05$ .

48 and 72 h, honokiol induced 39% and 48% of neuro-2a cells to undergo apoptosis.

*Honokiol Increases Levels of Bax and its Translocation from the Cytoplasm to Mitochondria*

Exposure of neuro-2a cells to 40  $\mu$ M honokiol for 24 h augmented levels of proapoptotic Bax protein (Fig. 5).

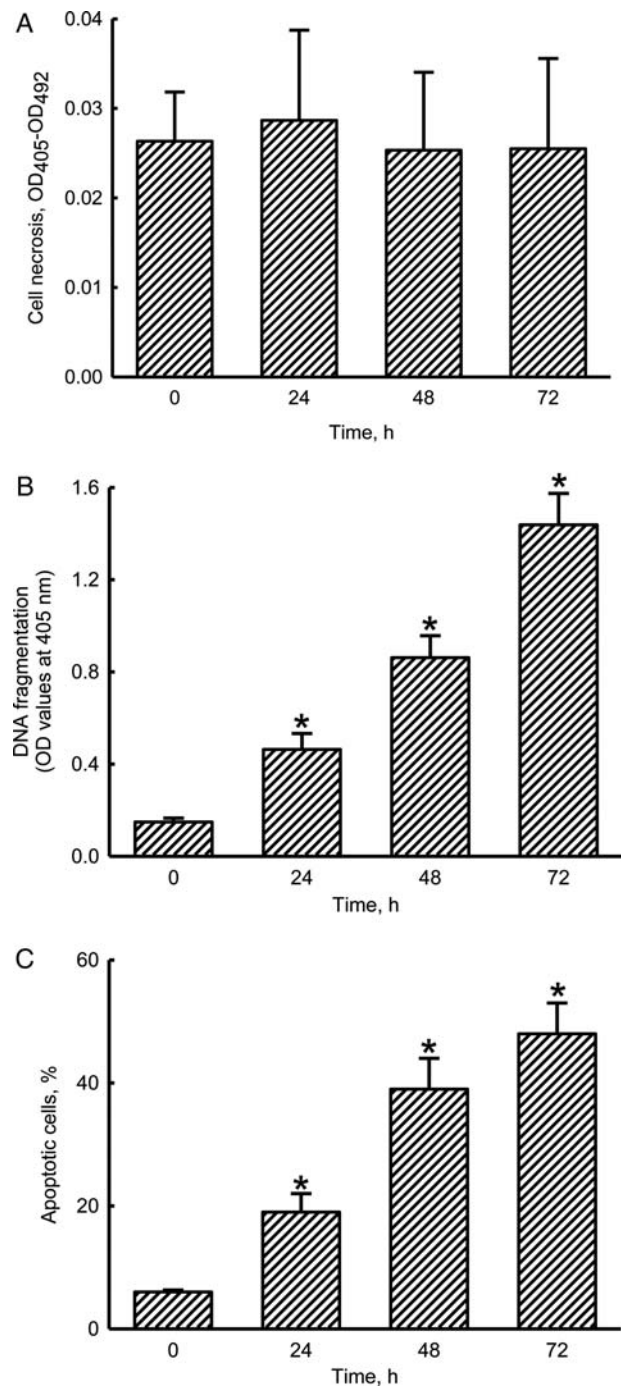


Fig. 4. Effects of honokiol on cell necrosis, DNA fragmentation, and cell apoptosis. Neuro-2a cells were treated with 40  $\mu$ M honokiol for 24, 48, and 72 h. Cell necrosis was assayed using a photometric immunoassay (A). DNA fragmentation was quantified with a cellular DNA fragmentation ELISA kit (B). Apoptotic cells were determined using flow cytometry (C). Each value represents the mean  $\pm$  standard error of the mean for  $n = 6$ . \*The value significantly differs from the respective control,  $P < .05$ .

After treatment for 48 and 72 h, amounts of Bax time-dependently increased. Mitochondria were stained using the DiOC<sub>6</sub> dye. Treatment of neuro-2a cells with 40  $\mu$ M honokiol for 24, 48, and 72 h obviously



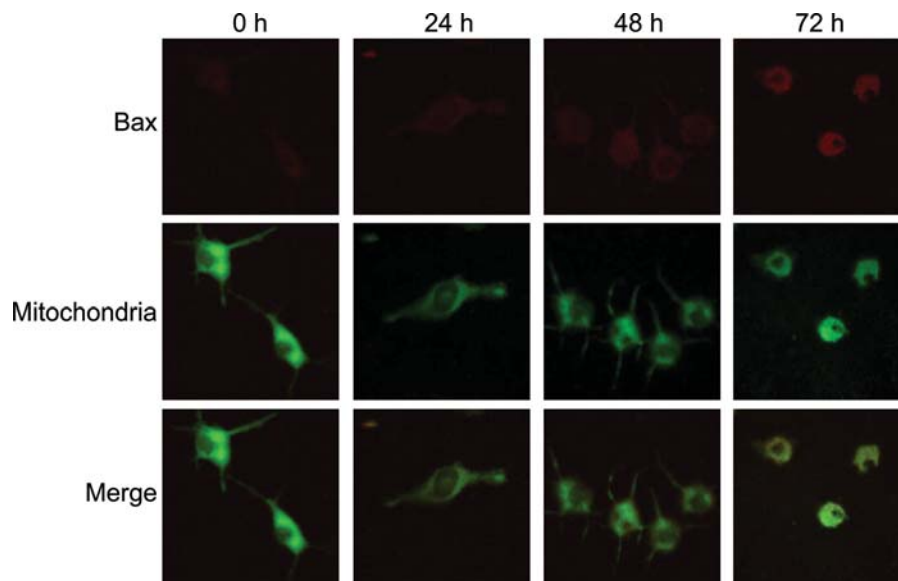


Fig. 5. Effects of honokiol on the translocation of Bax from the cytoplasm to mitochondria. Neuro-2a cells were treated with 40  $\mu\text{M}$  honokiol for 24, 48, and 72 h. The distribution of Bax protein in neuro-2a cells was immunodetected using an antibody with Cy3-conjugated streptavidin (*top panels*). Mitochondria of mouse cerebral endothelial cells (CECs) were stained with 3,3'-dihexyloxycarbocyanine (DiOC<sub>6</sub>), a positively charged dye (*middle panels*). The merged signals indicated that the Bax protein had been translocated into mitochondria (*bottom panels*).

decreased signals in mitochondria. The merged signals revealed that honokiol enhanced the translocation of Bax from the cytoplasm to mitochondria in a time-dependent manner.

#### *Honokiol Decreases the Mitochondrial Membrane Potential but Increases the Release of Cyt c*

Treatment of neuro-2a cells with 40  $\mu\text{M}$  honokiol for 24 h decreased the mitochondrial membrane potential by 14% (Fig. 6A). When the administered intervals reached 48 and 72 h, honokiol caused 25% and 37% reductions in the mitochondrial membrane potential. Exposure of neuro-2a cells to honokiol for 24 h increased the levels of Bax (Fig. 6B). After treatment for 48 and 72 h, honokiol augmented greater amounts of cellular Cyt c (lanes 3 and 4). Amounts of  $\beta$ -actin were immunodetected as the internal control (Fig. 6B). These immunorelated protein bands were quantified and analyzed (Fig. 6C). Treatment of neuro-2a cells with honokiol for 24, 48, and 72 h increased the levels of Cyt c by 2.2-, 2.8-, and 2.1-fold, respectively.

#### *Honokiol Stimulates Cascade Activation of Caspases-9, -3, and -6*

Exposure of neuro-2a cells to 40  $\mu\text{M}$  honokiol for 24 h increased caspase-9 activity by 67% (Fig. 7A). After exposure for 48 and 72 h, caspase-9 activities were significantly augmented by 2.5- and 2.4-fold, respectively. Similarly, treatment with honokiol for 24 h caused a significant 65% elevation in caspase-3 activity (Fig. 7B). Caspase-3 activities were time-dependently enhanced

by 2.1-fold and 91% following exposure for 48 and 72 h, respectively. After treatment with honokiol for 24, 48, and 72 h, caspase-6 activities in neuro-2a cells were significantly increased by 71%, 2.1-fold, and 80% (Fig. 7C). When neuro-2a cells were pretreated with Z-VEID-FMK, an inhibitor of caspase-6, for 1 h, honokiol-enhanced activation of caspase-6 was significantly reduced by 33% (Fig. 7D). In parallel, honokiol-induced DNA fragmentation and cell apoptosis were alleviated by 48% and 30% following pretreatment with a caspase-6 inhibitor (Fig. 7E and F).

#### *Honokiol Did Not Cause Insults to Mouse CECs and Human Astrocytes but Induces Apoptosis of the Other Mouse Neuroblastoma NB41A3 Cells*

Exposure of mouse CECs and human HA-h astrocytes to 40  $\mu\text{M}$  honokiol for 72 h did not affect cell viability and cell apoptosis (Table 1). In comparison, treatment of neuroblastoma NB41A3 cells with 40  $\mu\text{M}$  honokiol caused a significant 44% decrease in cell viability (Table 1). In parallel, honokiol at 40  $\mu\text{M}$  induced apoptosis of NB41A3 cells by 48%.

## Discussion

This study shows that honokiol passed through the CEC-constructed tight-junction barrier and induced insults to neuroblastoma cells. Analyses by HPLC and the UV spectrum revealed that honokiol can pass through the CEC-constructed tight-junction barrier. In parallel, exposure of neuroblastoma neuro-2a cells and NB41A3 cells to honokiol induced cell death.



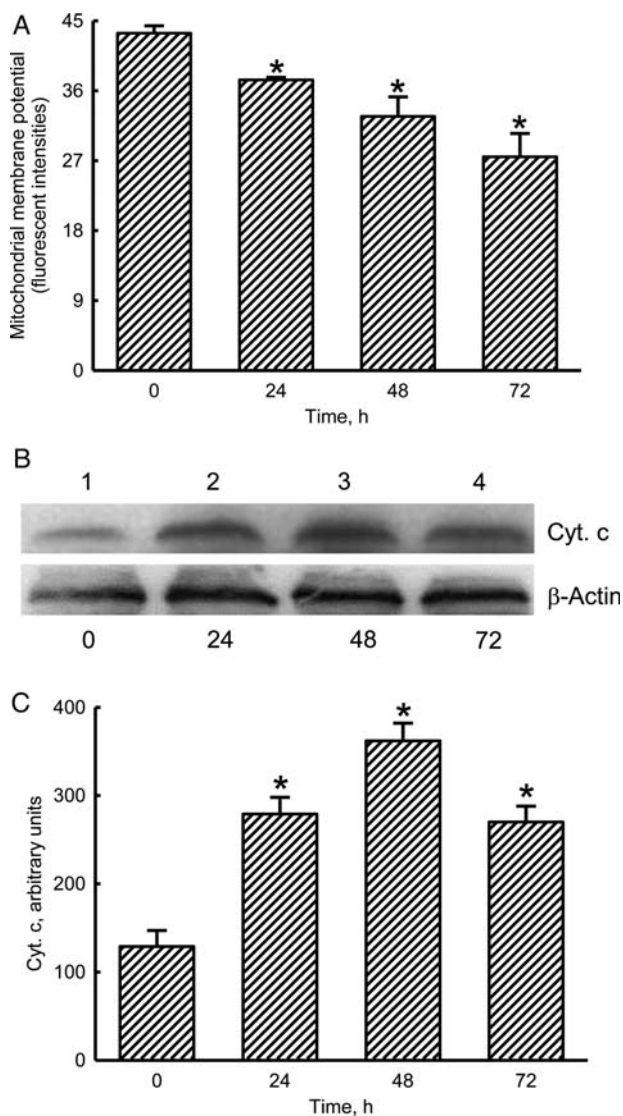


Fig. 6. Effects of honokiol on the mitochondrial membrane potential and cytochrome (Cyt) c release. Neuro-2a cells were treated with 40  $\mu$ M honokiol for 24, 48, and 72 h. The mitochondrial membrane potential was quantified using flow cytometry (A). Levels of Cyt c were immunodetected (B, top panel). Amounts of  $\beta$ -actin were measured as the internal control (bottom panels). These immunorelated protein bands were quantified and analyzed (C). Each value represents the mean  $\pm$  standard error of the mean for  $n = 6$ . \*The value significantly differs from the respective control,  $P < .05$ .

Neuroblastoma is an embryonal cancer of the sympathetic nervous system and often occurs in young children.<sup>2</sup> Because children with a neuroblastoma are usually designated as high-risk patients,<sup>3</sup> this cancer has become a major problem in pediatric oncology. Traditionally, therapies for treating neuroblastomas include a coordinated sequence of chemotherapy, surgery, and radiation.<sup>4</sup> However, these means may produce serious adverse effects, such as hearing loss, cardiac dysfunction, infertility, and second malignancies.<sup>5,6</sup> In a preclinical model, honokiol was shown to

have a variety of outcomes on antiangiogenesis, anti-inflammation, and anti-tumorigenesis but not to induce appreciable toxicity.<sup>13</sup> The present study further showed that honokiol can traverse the BBB and induce death of neuroblastoma cells. As well, our ongoing study further showed that honokiol at even low concentrations  $<10 \mu$ M could protect mouse CECs against ischemia/reperfusion-induced cell death (data not shown). Therefore, honokiol alone or in combined treatment with other conventional techniques may provide more-effective but less-toxic therapy for cranial or noncranial neuroblastoma.

Honokiol can pass through the BBB. This study showed that CECs used in this study could form a tight-junction barrier. Our previous study performed an immunocytochemical analysis to identify that CECs are specialized endothelial cells from cerebrovessels.<sup>29</sup> When CECs were cultured at a high density for 4 days, these specialized endothelial cells formed compact morphologies and expressed the ZO-1 protein. ZO-1 is a typical tight-junction protein that participates in CEC-involved construction of the BBB.<sup>41</sup> Furthermore, our permeability assay demonstrated that the CEC-constructed tight-junction barrier could obstruct the passing of the large molecule FITC-dextran. Another study done in our laboratory also showed that the tight-junction barrier could maintain a constant transendothelial electric resistance.<sup>31</sup> Obstruction against the passage of FITC-dextran and maintenance of transendothelial electric resistance are distinctive characteristics of the BBB assembly.<sup>31,42</sup> Therefore, all of our present data support the successful establishment of an in vitro CEC-built tight-junction barrier. Analysis by HPLC revealed that, when honokiol was added to the upper layer of the transwells, this polyphenol was detected in the bottom medium and had the same UV spectrum as that of standard honokiol. In addition, this study has further shown that honokiol can pass through the BBB of ICR mice. Thus, our results reveal that honokiol can cross the CEC tight-junction barrier and the BBB. Therapeutic options for treatment of malignant brain tumors are limited because of the presence of the BBB.<sup>17</sup> Therefore, honokiol may be an effective candidate drug for treating brain tumors because of its characteristic of traversing the BBB.

Honokiol induces death of neuroblastoma cells via an apoptotic mechanism. Exposure of neuro-2a cells and NB41A3 cells to honokiol provoked cell shrinkage and decreased cell viability. The  $LC_{50}$  of honokiol to neuroblastoma cells was  $\sim 63 \mu$ M. Honokiol was shown to have potent cytotoxicity to tumor cells, including leukemia, lung cancer, and hepatoma.<sup>13</sup> This study provides in vitro data to further demonstrate the effects of honokiol in damaging neuroblastoma cells. After exposure to 40  $\mu$ M honokiol, the fractions of neuro-2a cells suffering DNA fragmentation and arrest at the sub-G1 phase significantly increased. Cell shrinkage, DNA fragmentation, and cell cycle arrest at the sub-G1 phase are typical characteristics of cells undergoing apoptosis.<sup>22,30</sup> In addition, the results by a necrotic analysis revealed that honokiol did not cause necrosis of neuro-2a cells. As a result,

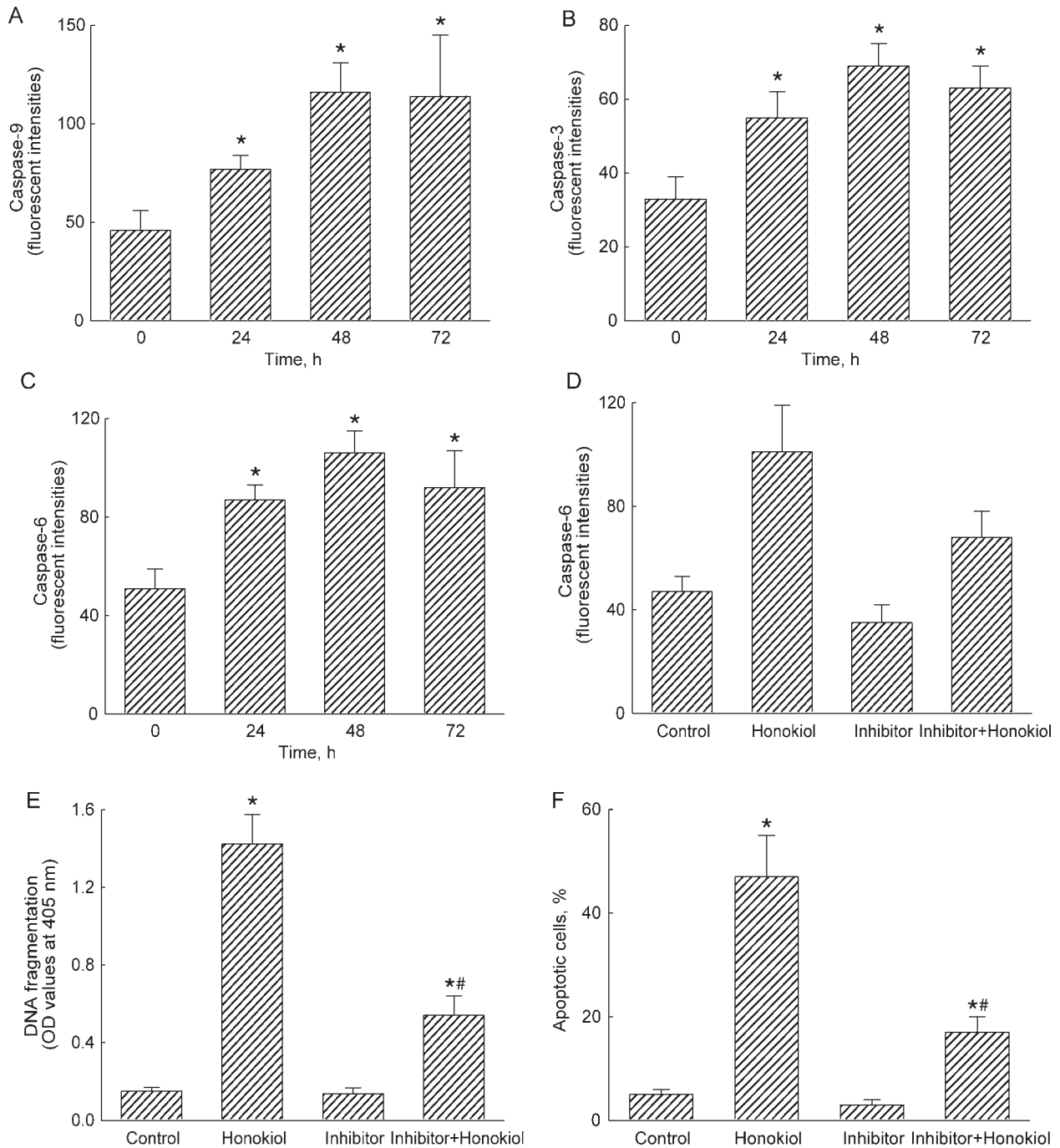


Fig. 7. Effects of honokiol on activities of caspases-9, -3, and -6. Neuro-2a cells were treated with 40  $\mu$ M honokiol for 24, 48, and 72 h. Activities of caspase-9, -3, and -6 were analyzed by fluorogenic assays using LEHD, DEVD, and VEID as the substrates, respectively (A–C). Neuro-2a cells were pretreated with 50  $\mu$ M Z-VEID-FMK, an inhibitor of caspase-6, for 1 h, and then exposed to honokiol. Caspase-6 activity was assayed using a fluorogenic method (D). DNA fragmentation was quantified using a BrdU-labeled histone-associated enzyme-linked immunosorbent assay kit (E). Apoptotic cells were quantified using flow cytometry (F). Each value represents the mean  $\pm$  standard error of the mean for  $n = 6$ . \* A value significantly ( $P < .05$ ) differs from the respective control group. # A value significantly ( $P < .05$ ) differs from the respective honokiol-treated group.

honokiol can lead to death of neuroblastoma cells through an apoptotic mechanism. In comparison, this study showed that honokiol did not induce insults to non-neoplastic cells, including mouse CECs and human astrocytes. A drug that can target cell death

through an apoptotic pathway was described as an effective candidate for cancer therapy.<sup>21</sup> For instance, Bcl-2 family proteins are apoptosis-related proteins and play important roles in the development of head and neck cancers. Discovering certain drugs that can

**Table 1.** Effects of honokiol on insults to mouse cerebral endothelial cells (CECs), human astrocytes (HA-h), and mouse neuroblastoma cells (NB41A3)

	Cell viability, Percentage of control		Apoptotic cells, %	
	Control	Honokiol	Control	Honokiol
CECs	100	98 ± 11	5 ± 1	6 ± 2
HA-h	100	92 ± 13	6 ± 1	8 ± 2
NB41A3	100	56 ± 16 <sup>a</sup>	5 ± 2	48 ± 8 <sup>a</sup>

Exposure of mouse CECs, HA-h cells, and NB41A3 cells to 40  $\mu$ M honokiol for 72 h. Cell viability was assayed using a colorimetric method. Apoptotic cells were quantified using a flow cytometer. Each value represents the mean  $\pm$  SEM for  $n = 6$ .

<sup>a</sup>The value significantly differs from the respective control,  $P < .05$ .

specifically inhibit the expression and activation of Bcl-2-related proteins was consequently implicated in improving the efficacy of Bcl-2-targeted therapy for treatment of head and neck squamous cell carcinoma.<sup>43</sup> Therefore, the effects of honokiol on inducing apoptosis of neuroblastoma cells, rather than necrosis, display its potential as an anticancer drug for treating brain tumors.

Bax protein is involved in honokiol-induced apoptotic insults to neuroblastoma cells. Treatment of neuro-2a cells with honokiol increased levels of Bax and simultaneously enhanced the translocation of this proapoptotic protein from the cytoplasm to mitochondria. Translocation of Bax to mitochondrial membranes can permeabilize the outer membrane.<sup>25</sup> In this study, depolarization of the mitochondrial membrane was verified by a reduction in the membrane potential of mitochondria of neuro-2a cells following exposure to honokiol. Therefore, the decrease in the mitochondrial membrane potential was attributable to honokiol-induced depolarization of the membrane. In parallel, after exposure to honokiol, levels of cytosolic Cyt c were significantly elevated. Cyt c is an apoptosis-related protein that can be released from mitochondria following apoptotic stimuli.<sup>26</sup> As a result, the honokiol-involved translocation of Bax and subsequent depolarization of the mitochondrial membrane potentially contribute to the release of Cyt c. There are 2 distinguishing intrinsic and extrinsic pathways that participate in regulating cell apoptosis.<sup>22,23</sup> A previous study showed that honokiol induced extrinsic death receptor-mediated apoptosis of human lung cancer cells by preferentially inhibiting the cellular FLICE-inhibitory protein.<sup>21</sup> This study further validates the intrinsic mechanism of honokiol-induced apoptotic insults to neuroblastoma cells from the viewpoint of a Bax-mitochondrion-Cyt c-dependent pathway.

Honokiol triggers cascade activation of caspase-9, -3, and -6. Exposure of neuro-2a cells to honokiol increased caspase-9 activity in a time-dependent manner. Caspase-9, an upstream protease in the process of intrinsic apoptosis, can be activated by a complex of Cyt c and apoptotic protease-activating factor-1.<sup>44</sup> The amounts

of cytosolic Cyt c were obviously augmented in neuro-2a cells following honokiol treatment. Therefore, activation of caspase-9 in honokiol-treated neuro-2a cells is as a result of Cyt c release from mitochondria. Sequentially, honokiol enhanced caspase-3 activity in neuro-2a cells. Activation of caspase-9 is essential for proteolytic maturation of caspase-3.<sup>30,44</sup> After activation, caspase-3 can cleave cellular key proteins, such as lamin and nuclear mitotic apparatus proteins, to affect cell functions.<sup>26</sup> Perifosin, an AKT inhibitor, showed in vitro and in vivo inhibition of neuroblastoma tumor cell growth through a caspase-3-dependent pathway.<sup>45</sup> This study also revealed that honokiol could turn on caspase-6 activity. Caspase-3 has a chronological effect on activation of caspase-6.<sup>22,29</sup> Thus, the honokiol-caused enhancement of caspase-6 activity is attributable to cascade activation of caspase-9 and -3. In comparison, when caspase-6 activity was suppressed by its specific inhibitor Z-VEID-FMK, honokiol-induced DNA fragmentation and apoptosis of neuro-2a cells were significantly attenuated. Therefore, the honokiol-induced cascade activation of caspases-9, -3, and -6 contributes to the induction of apoptotic insults to neuroblastoma cells.

In summary, the present study showed that honokiol could traverse the CEC-constructed tight-junction barrier and the BBB of ICR mice. In parallel, honokiol decreased viabilities of neuro-2a cells, and its LC<sub>50</sub> was determined to be 63  $\mu$ M. Exposure of neuroblastoma neuro-2a cells and NB41A3 cells to 40  $\mu$ M honokiol induced cell shrinkage, DNA fragmentation, or cell apoptosis. In comparison, honokiol did not trigger necrosis of neuroblastoma cells. Honokiol enhanced translocation of Bax from the cytoplasm to mitochondria and, consequently, induced alterations in the mitochondrial membrane potential and Cyt c release. After exposure to honokiol, the activities of caspase-9, -3, and -6 were sequentially activated. Reducing caspase-6 activity caused significant improvement of honokiol-induced DNA fragmentation and cell apoptosis. Taken together, this study showed that honokiol can pass through the CEC tight-junction barrier and induce apoptotic insults to neuroblastoma cells via a Bax-mitochondrion-Cyt c-caspase protease pathway. Subsequent translational studies on whether honokiol can suppress the growth of neuroblastoma in null mice are being performed in our laboratory. In addition, we are interested to investigate whether honokiol can treat patients with neuroblastoma with commonly used anti-tumor drugs, such as doxorubicin, cyclophosphamide, and etoposide, to reduce the adverse effects induced by these drugs.

## Acknowledgments

We thank Ivy Tsai and Huei-San Shie for skillful technical assistance.

*Conflict of interest statement.* None declared.



## Funding

This study was supported by grants from Taipei Medical University-Shuang Ho Hospital (98TMU-

SHH-09), Wan-Fang Hospital (100-WF-EVA-002), the Department of Health (DOH97-NNB-1037; DOH100-TD-C-111-008), and the National Science Council (95-2745-B-038-001-URD), Taipei, Taiwan.

## References

- van der Pal HJ, van Dalen EC, Kremer LC, et al. Risk of morbidity and mortality from cardiovascular disease following radiotherapy for childhood cancer: a systematic review. *Cancer Treat Rev.* 2005;31:173–185.
- Hoehner JC, Gestblom C, Hedborg F, et al. A developmental model of neuroblastoma: differentiating stroma-poor tumors' progress along an extra-adrenal chromaffin lineage. *Lab Invest.* 1996;75:659–675.
- Park JR, Eggert A, Caron H. Neuroblastoma: biology, prognosis, and treatment. *Pediatr Clin North Am.* 2008;55:97–120.
- Pearson AD, Pinkerton CR, Lewis IJ, et al. European Neuroblastoma Study Group, Children's Cancer and Leukaemia Group (CCLG formerly United Kingdom Children's Cancer Study Group). High-dose rapid and standard induction chemotherapy for patients aged over 1 year with stage 4 neuroblastoma: a randomised trial. *Lancet Oncol.* 2008;9:247–256.
- Laverdière C, Cheung NK, Kushner BH, et al. Long-term complications in survivors of advanced stage neuroblastoma. *Pediatr Blood Cancer.* 2005;45:324–332.
- Zage PE, Kletzel M, Murray K, et al. Children's Oncology Group. Outcomes of the POG 9340/9341/9342 trials for children with high-risk neuroblastoma: a report from the Children's Oncology Group. *Pediatr Blood Cancer.* 2008;51:747–753.
- Wagner LM, Danks MK. New therapeutic targets for the treatment of high-risk neuroblastoma. *J Cell Biochem.* 2009;107:46–57.
- Matthay KK, Villablanca JG, Seeger RC, et al. Treatment of high-risk neuroblastoma with intensive chemotherapy, radiotherapy, autologous bone marrow transplantation, and 13-cis-retinoic acid. *N Engl J Med.* 1999;341:1165–1173.
- Chen L, Zhang Q, Yang G, et al. Rapid purification and scale-up of honokiol and magnolol using high-capacity high-speed counter-current chromatography. *J Chromatogr A.* 2007;1142:115–122.
- Lo YC, Teng CM, Chen CF, et al. Magnolol and honokiol isolated from *Magnolia officinalis* protect rat heart mitochondria against lipid peroxidation. *Biochem Pharmacol.* 1994;47:549–553.
- Kotani H, Tanabe H, Mizukami H, et al. Identification of a naturally occurring rexinoid, honokiol, that activates the retinoid X receptor. *J Nat Prod.* 2010;73:1332–1336.
- Esumi T, Makado G, Zhai H, et al. Efficient synthesis and structure-activity relationship of honokiol, a neurotrophic biphenyl-type neolignan. *Bioorg Med Chem Lett.* 2004;14:2621–2625.
- Fried LE, Arbiser JL. Honokiol, a multifunctional antiangiogenic and antitumor agent. *Antioxid Redox Signal.* 2009;11:1139–1148.
- Zhai H, Nakade K, Oda M, et al. Honokiol-induced neurite outgrowth promotion depends on activation of extracellular signal-regulated kinases (ERK1/2). *Eur J Pharmacol.* 2005;516:112–117.
- Lin YR, Chen HH, Ko CH, et al. Neuroprotective activity of honokiol and magnolol in cerebellar granule cell damage. *Eur J Pharmacol.* 2006;537:64–69.
- Wang X, Duan X, Yang G, et al. Honokiol crosses BBB and BCSFB, and inhibits brain tumor growth in rat 9L intracerebral gliosarcoma model and human U251 xenograft glioma model. *PLoS One.* 2011;6:e18490.
- Doolittle ND, Anderson CP, Bleyer WA, et al. Importance of dose intensity in neuro-oncology clinical trials: summary report of the Sixth Annual Meeting of the Blood-Brain Barrier Disruption Consortium. *Neuro Oncol.* 2001;3:46–54.
- Engelhardt B. Development of the blood-brain barrier. *Cell Tissue Res.* 2003;314:119–129.
- Abbott NJ, Ronnback L, Hansson E. Astrocyte-endothelial interactions at the blood-brain barrier. *Nat Rev Neurosci.* 2006;7:41–53.
- Rubin LL. Endothelial cells: adhesion and tight junctions. *Curr Opin Cell Biol.* 1992;4:830–833.
- Raja SM, Chen S, Yue P, et al. The natural product honokiol preferentially inhibits cellular FLICE-inhibitory protein and augments death receptor-induced apoptosis. *Mol Cancer Ther.* 2008;7:2212–2223.
- Goyal L. Cell death inhibition: keeping caspases in check. *Cell.* 2001;104:805–808.
- Chen RM, Chen TL, Chiu WT, et al. Molecular mechanism of nitric oxide-induced osteoblast apoptosis. *J Orthop Res.* 2005a;23:462–468.
- Pagliari LJ, Kuwana T, Bonzon C, et al. The multidomain proapoptotic molecules Bax and Bak are directly activated by heat. *Proc Natl Acad Sci USA.* 2005;102:17975–17980.
- Saikumar P, Dong Z, Patel Y, et al. Role of hypoxia-induced Bax translocation and cytochrome c release in reoxygenation injury. *Oncogene.* 1998;17:3401–3415.
- Rao L, Perez D, White E. Lamin proteolysis facilitates nuclear events during apoptosis. *J Cell Biol.* 1996;135:1441–1455.
- Jiang QQ, Fan LY, Yang GL, et al. Improved therapeutic effectiveness by combining liposomal honokiol with cisplatin in lung cancer model. *BMC Cancer.* 2008;8:242.
- Xu J, Yeh CH, Chen S, et al. Involvement of de novo ceramide biosynthesis in tumor necrosis factor- $\alpha$ /cycloheximide-induced cerebral endothelial cell death. *J Biol Chem.* 1998;273:16521–16526.
- Chen TG, Chen TL, Chang HC, et al. Oxidized low-density lipoprotein induces apoptotic insults to mouse cerebral endothelial cells via a Bax-mitochondria-caspase protease pathway. *Toxicol Appl Pharmacol.* 2007;219:42–53.
- Chang HC, Chen TG, Tai YT, et al. Resveratrol attenuates oxidized LDL-evoked Lox-1 signaling and consequently protects against apoptotic insults to cerebrovascular endothelial cells. *J Cereb Blood Flow Metab.* 2011;31:842–854.
- Lin YL, Chang HC, Chen TL, et al. Resveratrol protects against oxidized LDL-induced breakage of the blood-brain barrier by lessening disruption of tight junctions and apoptotic insults to mouse cerebrovascular endothelial cells. *J Nutr.* 2010;140:2187–2192.
- Tang W, Wan M, Zhu Z, et al. Simultaneous determination of eight major bioactive compounds in Dachengqi Tang (DT) by high-performance liquid chromatography. *Chinese Med.* 2008;3:5.
- Huang TY, Chen TL, Liao MH, et al. *Drynaria fortunei* J. Sm. promotes osteoblast maturation by inducing differentiation-related gene expression and protecting against oxidative stress-induced apoptotic insults. *J Ethnopharmacol.* 2010;131:70–77.

34. Chen RM, Chen TL, Lin YL, et al. Ketamine reduces nitric oxide biosynthesis in human umbilical vein endothelial cells through downregulating endothelial nitric oxide synthase expression and intracellular calcium levels. *Crit Car Med*. 2005;33:1044–1049.
35. Chang CC, Liao YS, Lin YL, et al. Nitric oxide protects osteoblasts from oxidative stress-induced apoptotic insults via a mitochondria-dependent mechanism. *J Orthop Res*. 2006;24:1917–1925.
36. Wu GJ, Chen TG, Chang HC, et al. Nitric oxide from both exogenous and endogenous sources activates mitochondria-dependent events and induces insults to human chondrocytes. *J Cell Biochem*. 2007;101:1520–1531.
37. Tai YT, Cherng YG, Chang CC, et al. Pretreatment with low nitric oxide protects osteoblasts from high nitric oxide-induced apoptotic insults through regulation of c-Jun N-terminal kinase/c-Jun-mediated *Bcl-2* gene expression and protein translocation. *J Orthop Res*. 2007;25:625–635.
38. Cherng YG, Chang HC, Lin YL, et al. Apoptotic insults to human chondrocytes induced by nitric oxide are involved in sequential events, including cytoskeletal remodeling, phosphorylation of mitogen-activated protein kinase kinase kinase-1, and Bax-mitochondria-mediated caspase activation. *J Orthop Res*. 2008;26:1018–1026.
39. Ho WP, Chan WP, Hsieh MS, et al. Runx2-mediated *Bcl-2* gene expression contributes to nitric oxide protection against oxidative stress-induced osteoblast apoptosis. *J Cell Biochem*. 2009;108:1084–1093.
40. Chen RM, Lin YL, Chou CW. GATA-3 transduces survival signals in osteoblasts through upregulation of *bcl-x<sub>L</sub>* gene expression. *J Bone Min Res*. 2010;25:2193–2204.
41. Huber JD, Egleton RD, Davis TP. Molecular physiology and pathophysiology of tight junctions in the blood-brain barrier. *Trends Neurosci*. 2001;24:719–725.
42. Siddharthan V, Kim YV, Liu S, et al. Human astrocytes/astrocyte-conditioned medium and shear stress enhance the barrier properties of human brain microvascular endothelial cells. *Brain Res*. 2007;1147:39–50.
43. dos Santos LV, Carvalho AL. Bcl-2 targeted-therapy for the treatment of head and neck squamous cell carcinoma. *Recent Pat Anticancer Drug Discov*. 2011;6:45–57.
44. Garrido C, Galluzzi L, Brunet M, et al. Mechanisms of cytochrome c release from mitochondria. *Cell Death Differ*. 2006;13:1423–1433.
45. Li Z, Tan F, Liewehr DJ, et al. In vitro and in vivo inhibition of neuroblastoma tumor cell growth by AKT inhibitor perifosine. *J Natl Cancer Inst*. 2010;102:758–770.